# Modeling the mechanism of compensation of aberrations in the human eye for accommodation and aging

**Juan Tabernero,* Esther Berrio, and Pablo Artal**

*Laboratorio de Optica, Instituto Universitario de investigación en Óptica y Nanofísica (IUiOyN), Universidad de Murcia, Campus de Espinardo (Edificio 34) 30100 Murcia, Spain*
**Corresponding author: juant@um.es*

Received June 7, 2011; revised July 22, 2011; accepted July 22, 2011;
posted July 22, 2011 (Doc. ID 148447); published August 25, 2011

The mechanisms of compensation of aberration between cornea and lens are somehow modified during both accommodation and aging. In 15 individualized ocular models of young and unaccommodated eyes, we used morphological data of the lens to simulate the effect of accommodation and aging on these mechanisms. The predicted changes in aberrations were compared to data from the literature. In general, only the variation of the lens curvature was enough to reproduce the decrease in ocular spherical aberration (SA) during accommodation. However, the increase in SA with age could only be explained as a consequence of an increase in the conic constant of the lens and/or additional changes on the gradient index. 

*OCIS codes:* 330.0330, 330.7326, 330.7322, 330.7323.

## 1. INTRODUCTION

The optics of the human eye is partially optimized by minimizing spherical aberration (SA) and coma [1–6]. The mechanisms driving these effects seem to have different sources. The asphericities of the ocular surfaces and/or the crystalline lens gradient index probably play the main role in the balance of SA between the cornea and the crystalline lens. On the other hand, the curvatures of the surfaces, through the shape factor of both lenses, may be responsible for the compensation of the corneal horizontal coma by the lens [7].

Nevertheless, there are some situations where this fine balance of the ocular aberrations might be altered, either by artificial disruptive factors or naturally. Both refractive surgery acting on the cornea [8] and cataract surgery on the lens [9] are examples of artificial disruption. Although both procedures typically target for a null refractive outcome, recently the effect of higher-order aberrations is also being considered; for instance, new intraocular lenses for cataract surgery that preserve the natural balance of SA or coma were designed [9,10].

A second class of disruption factors are those related to naturally induced misbalances. Among the most relevant are accommodation, which induces a change of the lens curvatures and the subsequent variations of the optical properties, and aging, which is also associated to a number of structural ocular changes. In general, any effect on the parameters driving the mechanism of compensation of aberrations could be susceptible to alter the aberrations in the complete eye.

To address this problem, two different types of structural studies of the eye are presented in the literature. Some works use a geometrical approach to describe the variation of the ocular optics as a function of age and accommodation. They apply direct image methods (typically dealing with problems of optical distortions) to acquire data on the shape of the ocular surfaces [11–15]. Other studies measure the optical effects caused by these geometrical changes, i.e., how the aberrations of the ocular components change with age [16–24] and during accommodation [25–28].

However, a fundamental link connecting the results of both types of studies, the geometrical versus the optical changes, seems to be still unclear. A direct relationship between the causes and the effects of the ocular changes during aging and accommodation would help one to better understand the behavior of the optics of the eye and, eventually, might lead to the design of better solutions for optical ocular problems.

To further explore this problem, we use personalized optical models of young and nonaccommodated eyes [7]. We incorporated to them the geometrical changes occurring during accommodation and aging according to the averaged available data. The predicted aberration outcomes were compared to those from the literature. This allowed us to identify the critical factors mostly responsible for the potential variation in the ocular aberrations profile.

## 2. METHODS

In a previous publication, we developed a method to build up personalized optical models of the human eye [7]. Fifteen of these optical models of normal, young, and nonaccommodated eyes were used here (mean $\pm$ SD age: $22.3 \pm 2.0$). Briefly, the procedure consists of measuring the geometry of the first corneal surface (from corneal topography), the alignment of the optical elements of the eye (using our own research instrument based on recording the Purkinje images of the eye [29]), the axial length (with an optical biometer, IOL Master, Zeiss), and the wavefront aberrations of the eye (with our own research prototype of a Hartmann–Shack wavefront sensor [30]). Then, the anterior corneal surface was incorporated into a ray-tracing optical software (ZEMAX Development, San Diego, California, USA) as the first element

 

of a three surfaces optical model. The surfaces of the crystalline lens were initially taken from the Le Grand eye model [31]. In this step, the decentration and tilt of the lens measured with respect to the center of the pupil and the pupillary axis, respectively, were included in each model. Then, the models were optimized to reproduce the rotationally symmetrical terms of the wavefront aberration measured for each particular subject: defocus and SA. An optimization routine based on varying the radii of curvature and the asphericities of both lens surfaces was implemented to achieve this purpose. To evaluate the reliability of the method, the coma generated by each customized model was compared to the actual coma measured for that subject. In general, there was a good correlation between the predicted and the experimental horizontal coma for the whole set of subjects. The agreement analysis is presented in Fig. 1, which shows a direct correlation of the simulated versus measured data (left) and a plot of the differences against the mean value of the two values (right). There was no offset present (mean difference was 0.002 $\mu$m) and the standard deviation of the difference remained small enough (0.047 $\mu$m). This set of 15 individual eye models closely reproduce the quality of the normal, young, and nonaccommodated eye.

Taking the nonaccommodated situation as the starting point, accommodation was incorporated into the modeling by changing the curvatures of the crystalline lens according to data obtained from the literature. A similar approach was used to predict the optical changes that occurred with aging. Figure 2 shows a schematic diagram of the procedure.

Dubbelman *et al.* [13] provide a description of the changes in the shape of the crystalline lens that typically occur during accommodation. The ratios of change of the crystalline lens radii of curvature per accommodative (stimulus) diopter ($D$) were −0.61 mm/$D$ for the anterior surface and −0.13 mm/$D$ for the posterior surface. These changes were incorporated to every eye model in steps of a quarter of diopter up to 7$D$. We assumed that corneal aberrations and ocular alignment did not change during accommodation. Then, the wavefront aberration was calculated for every accommodative step, for an entrance pupil diameter of 5 mm. Besides, the possible effect of a variation in asphericity as the accommodative state of the model increased was also accounted for. A rate of −0.5 units of asphericity of the anterior lens surface per accommodative diopter (the lens becomes flatter in the periphery when accommodates) was also incorporated [13].

Concerning aging, our simulations included three simple geometrical changes of the lens. The surfaces of the crystalline lens suffered an increase in curvature, inducing more optical power that was at least partially compensated by a continuous growing of the lens and a decrease of the equivalent refractive index. We used the ratios given by Dubbelman *et al.* [12,14]: −0.057 mm/yr and −0.012 mm/yr for the decrease of the radii of curvature of the anterior and posterior lens surfaces, respectively, 0.024 mm/yr for the increase in lens thickness, and a decrease of −0.00039 per year of the equivalent refractive index. Again, we assumed that the cornea did not change much with age [32,33] and that nonsignificant variations in the alignment of the ocular surfaces and angle kappa occur with senescence [24]. The wavefront aberrations were calculated every ten years ranging from 20 to 80 years and for a 5 mm pupil diameter. Similarly to accommodation, we also evaluated the impact of a change in the asphericities of the crystalline lens surfaces with age. Although it is not so evident that such change exists, Dubbelman and Van der Heijde [12] measured a positive but not significant tendency of the asphericity to increase 0.03 per year for the anterior lens surface and 0.07 per year for the posterior lens surface (indicating that the periphery of the lens became more curved with age). For reasons that are exposed later in the discussion, we performed a second set of simulations incorporating these asphericity changes.

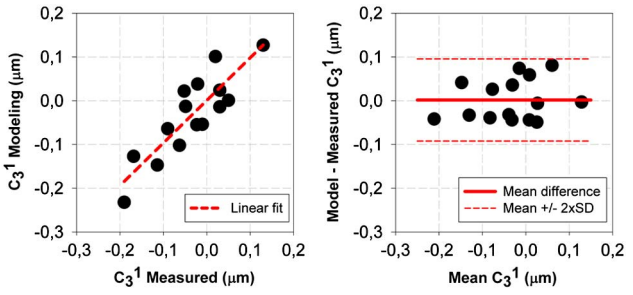


Fig. 1. (Color online) Predicted (from the models) versus measured horizontal coma ($C_3^1$) for the 15 eyes of the study (left plot). The difference between predictions and measurements are plotted against the average of the two values (right plot).

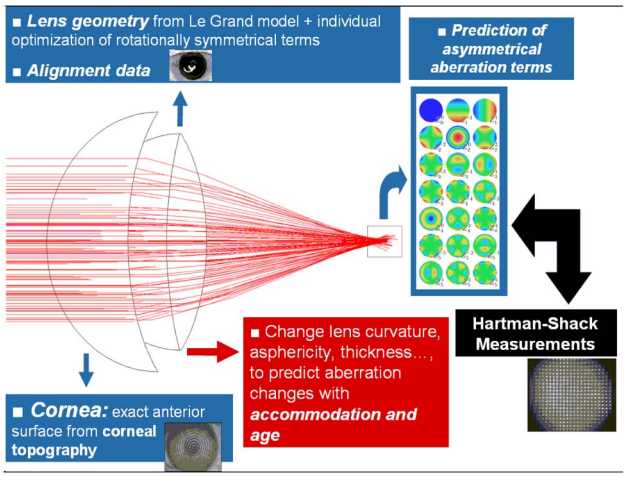


Fig. 2. (Color online) Schematic diagram of the procedure to build up the individualized eye models used in this work.

## 3. RESULTS

### A. Accommodation

Figure 3 shows the changes in SA and coma in the 15 eye models when the accommodation was increased up to 7$D$, changing only lens curvatures. The solid and thicker lines represent the average of the 15 eyes. As expected, SA changed in the negative direction with the increase in the accommodation stimulus for all tested eyes. However, the direction of the comatic change with accommodation was more variable across the different eyes. On average, there was a very small increment in the negative direction. Figure 4 shows the effect of adding a negative change of asphericity to the anterior surface of the crystalline lens, as measured by Dubbelman *et al.* [13] (−0.5 units/D). The solid curve shows the previous average data from Fig. 3(a), and the dotted line represents the newly calculated average from the 15 eye models when also the asphericity changed with accommodation. Solid thin lines

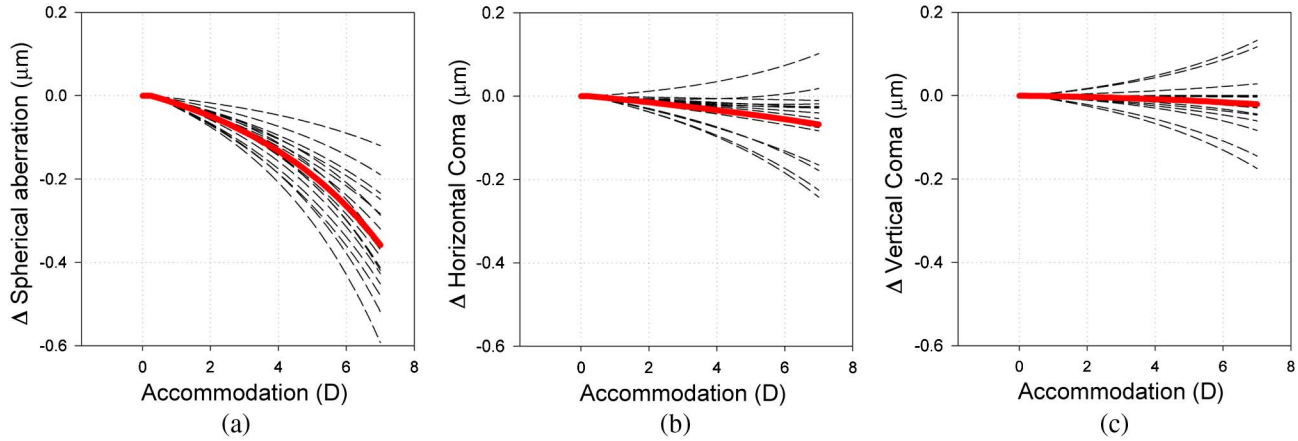


Fig. 3. (Color online) Changes in (a) SA and (b), (c) coma for the 15 eye models considered in the study when the accommodation stimulus was "virtually" increased up to 7 D, changing only lens curvatures.

represent the interval containing the mean values ± a standard deviation from the mean, reflecting the interindividual variability of the changes of SA with accommodation. The effect of the peripheral flattening of the anterior lens surface was reflected in an increase of the SA of the eye toward more negative values (peripheral rays focusing behind central rays). The magnitude of the change in SA due to the effect of asphericity was the order of 25%. Both results were compared to the experimental values measured by Cheng *et al.* [26] in 74 students. The straight solid line of Fig. 4 represents the linear tendency of the SA (pupil set to 5 mm diameter) obtained by Cheng *et al.* The tendency was in good agreement with our predictions and falls well in between the standard deviation interval of the prediction performed with aspherical changes on the lens. Cheng *et al.* also measured small changes in coma

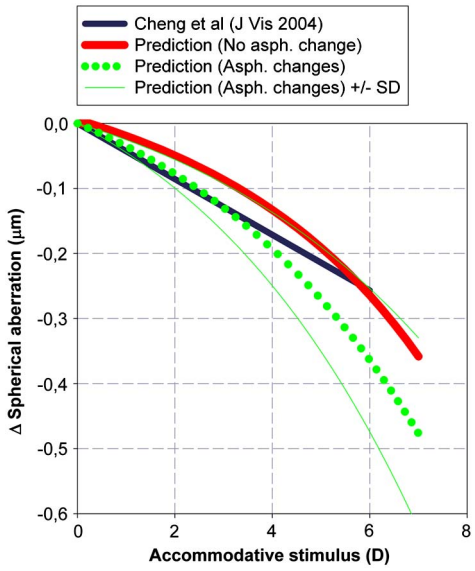


Fig. 4. (Color online) Changes in SA as a function of the accommodation stimulus. Solid curved line represents the average data of Fig. 3 (a) (changes in the crystalline lens surfaces included curvature but not asphericity). Dotted curved line represents the average data from the 15 eye models when asphericity was also allowed to change as a function of the accommodation level. The thin solid lines represents the standard deviation interval from the mean changes for this last predictive case. Solid straight line represents the experimental tendency measured in 74 subjects by Cheng *et al.* [26]. The data were all calculated for a fixed 5 mm pupil diameter.

but without a clearly defined tendency, in line with our predictions of Figs. 3(b) and 3(c).

Figure 5 shows the average value of the SA for three different accommodative states, at 0 (measured values), 3, and 6*D*, respectively (predicted values without asphericity change). On the left side column, the mean corneal SA was plotted (it did not change with accommodation based on the hypothesis used for the modeling procedure). The right side column represented the mean SA of the complete eye. On the central column, the internal aberration values, obtained from the direct subtraction of the corneal values to the ocular values, are shown. The internal values were already negative for the nonaccommodative state, and they changed toward a more negative contribution with the increase in accommodation. The eye, with initial positive SA values, experienced a sign reverse of SA during accommodation. The compensation of SA remained active during accommodation in the sense that, at every accommodative state, the internal and corneal values had opposite signs, and the eye had less SA than each of its optical components. A similar scheme was calculated for coma (not shown here for simplicity), but the small internal changes of coma with accommodation barely affected the compensation effect.

### B. Aging

Figure 6 shows the results of the SA variation with age. The solid line in Fig. 6(a) (prediction 1 in the legend) represents the variation of the mean predicted ocular SA of the 15 eye models when the crystalline lens changed its curvature, thickness, and equivalent refractive index according to previous studies. The geometrical changes induced a decrease of SA with age. However, different studies that performed noninvasive measurements in the living eye [21–24] reported a

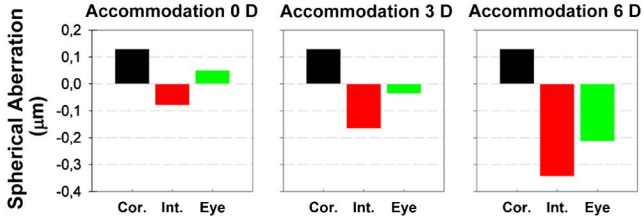


Fig. 5. (Color online) Average SA of the cornea, internal (crystalline lens), and total eye for three different accommodative states (infinity, 3 D, and 6 D). Pupil diameter was 5 mm.

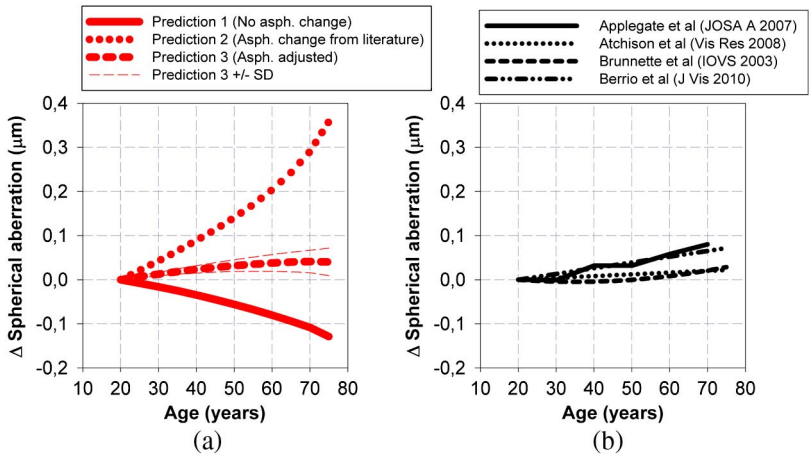


Fig. 6. (Color online) Comparison between (a) simulated data and (b) experimental data from the literature for the ocular SA as a function of age. The simulations included three different approaches to the rate of change in asphericity. Prediction 1 did not include changes in asphericity with age. Prediction 2 took a positive change in asphericity from Dubbelman and Van der Heijde's work [12]. Prediction 3 included a positive change but reduced by half compared to prediction 2. Standard deviation intervals from the mean value are also shown in the case of prediction 3. Pupil diameter was 5 mm for all data presented here.

positive change of ocular SA with age [Fig. 6(b)]. Trying to reproduce these empirical data, a second set of simulations were performed, this time incorporating a positive change of the conic constant of the anterior and posterior lens surfaces [12] (0.03 per year for the anterior surface and 0.07 per year for the posterior surface, i.e., the surfaces became more curved in the periphery). Including this factor in the simulations, the results effectively presented an increase in the ocular SA as a function of age [Fig. 6(a), dotted curve, prediction 2), but certainly too large when compared to the experimental values of Fig. 6(b). Given the uncertainty about the magnitude of the changes of asphericity with age, if any, since there is a clear lack of data in the literature, and with the purpose of estimate the effects on aberrations of different rates of changes in asphericity, we performed a third set of simulations using a positive variation of half the variation rate that was measured by Dubbelmann *et al.* (0.015 per year for the anterior surface and 0.035 per year for the posterior surface. The results are shown in Fig. 6(a), labeled prediction 3 (dashed curved). For this third situation, we incorporated the intervals that include the mean value minus and plus the standard deviation of the mean change [thin dashed lines in Fig. 6(a)]. The comparison with the experimental data in Fig. 6(b) was more satisfactory in this situation and all tendencies would be included on the 95% confidence interval of the predicted changes.

A similar scheme was presented in Fig. 7 for the values of the ocular rms of coma. Figure 7(a) shows the average predictions from the three different aging-evolving models explained earlier, and Fig. 7(b) exhibits the results of three different experimental studies [21,22,24]. Prediction 1 (thick solid line) was obtained after changing the curvature, thickness, and equivalent refractive index of the crystalline lens. The effects produced were small but slightly on the direction of negative changes of the coma rms along senescence. Similarly to the case of SA, prediction 2 (dotted line) was obtained after incorporating in the model the asphericity changes taken from the literature. This resulted in positive changes of coma with age,

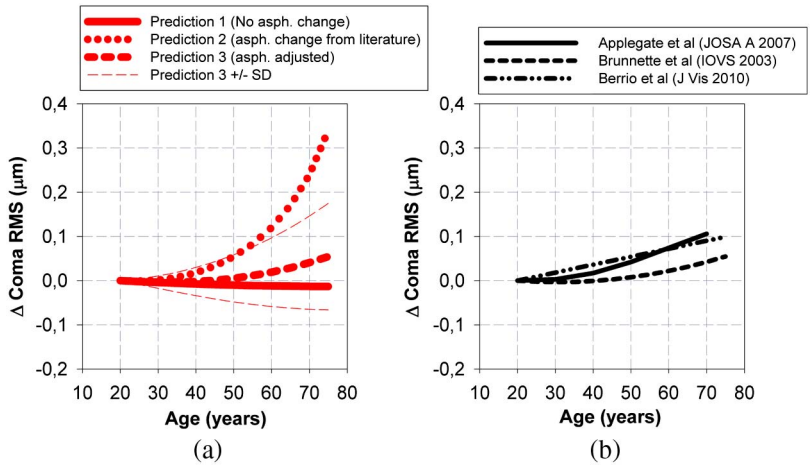


Fig. 7. (Color online) Comparison between (a) simulated data and (b) experimental data from the literature for the ocular coma rms as a function of age. The simulations included three different approaches to the change in asphericity. Prediction 1 did not include changes in asphericity with age. Prediction 2 took a positive change in asphericity from Dubbelman and Van der Heijde's work [12]. Prediction 3 included a positive change but reduced by half compared to prediction 2. Standard deviation intervals from the mean value are also shown in the case of prediction 3. Pupil diameter was 5 mm for all data presented here.

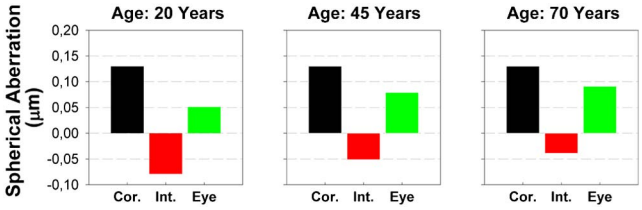


Fig. 8. (Color online) Average SA of the cornea, internal (crystalline lens), and total eye for three different ages (20, 45, and 75 years). Pupil diameter was 5 mm.

but again too large to be compared to the experimental results. Prediction 3 (dashed line) showed the results of changing lens asphericity as a ratio of half the one used for prediction 2. It also included the standard deviation interval from the mean change as in Fig. 6(a). This interval is now large compared to the one presented in 6A but it is a consequence of including the rms of two Zernike coefficients. As similar as in the SA case, prediction 3 presented the closest agreement with the experimental values of Fig. 7(b).

Figs. 8 shows the mean data for ocular SA compared to the mean corneal and crystalline lens SA. Data from prediction 3 (the one that provided the closest agreement with the experimental values) were used to test a possible disruption of the SA balancing effect. The left side bar represents the average corneal SA of the 15 subjects. This value remained constant with aging. The central bar shows the averaged SA of the crystalline lens, calculated as the direct subtraction of the corneal values to the ocular values. The bar on the right-hand side of the plots shows the ocular SA. This scheme was repeated three times for three different ages: 20, 45, and 70 years old estimations. At 20 years old, the values represents the average of the measurements, while, for 45 and 70 years old, the values incorporate the outcomes from prediction 3 in Fig. 6. These results suggest that a small decrease of the balance of SA between cornea and lens occurs with age, although both optical components still sustained opposite signs for SA. The estimated changes of coma presented in Fig. 7 also suggest a similar behavior for this aberration term.

## 4. DISCUSSION

### A. Change of Aberrations with Accommodation

It is well known that the SA of the eye changes to more negative values with accommodation, and several eye models have been proposed to reproduce it. An accommodating schematic eye [34] attempted to model the possible changes of asphericity and equivalent refractive index with accommodation. Although the model had some limitations to predict the average SA of the eye, it predicted the negative change of SA. Still, it was not clear how the different geometrical changes (curvature, asphericity, refractive index) contributed to the total negative variation of the SA. Given the dispersion of the actual experimental data [26], our results showed that variation of the radii of curvature of both lens surfaces was enough to predict reasonably well the decrease of SA with accommodation. Perhaps, a more accurate matching is possible when changes in the anterior lens asphericity are included (note that there is still a lack of data on the potential variation of the posterior lens asphericity). Considering the agreement obtained with the initial procedure (Fig. 4), additional optical changes affecting the lens during accommodation must have a minor effect for the lens SA variation. Potential changes on the gradient index structure of the lens during accommodation caused by small variations of the biomechanical properties of the lens fibers might be also inducing additional subtle changes in SA.

Since the change of the crystalline lens SA goes always in the negative direction when the eye accommodates, we should still expect some benefit from having a positive corneal SA (see Fig. 5). In this sense, accommodation cannot be considered, strictly, as a disruption factor of the mechanism of SA compensation between the cornea and the lens, since some SA balance is present at every accommodative state. Nonetheless, the magnitude of this beneficial balance decreases under a strong accommodation effort (Fig. 5, lower panel).

We also predicted some inconsistent changes in coma when the accommodation level increased, in line with previous experimental results. The origins of these changes are not well understood. Cheng *et al.* [26] suggested that a shift on the lens position during accommodation would explain the results. However, the simulations we performed kept the alignment properties of the eye as constants and, still, we obtained inconsistent data in the direction and magnitude of the change in coma. Therefore, an explanation unrelated to the alignment properties should be proposed. The Seidel primary aberrations theory for a thin lens predicts a change of coma directly proportional to the square of the optical power of the lens and linearly proportional to its shape factor [35]. These two variables suffer variations of opposite sign during accommodation. In particular, there is an increment of optical power and a decrease of the shape factor of the lens toward the zero value (i.e., a more equi-biconvex lens). At least two possible scenarios could be expected: one where the contribution of these factors to the coma aberration would cancel out each other, resulting in noncomalike changes in the eye with accommodation (which certainly occurred for many subjects), and one where some under/overcompensation effect of one factor with respect to the other would be presented. Depending on the initial values, this last situation would generate different directions in the comalike response to accommodation. Although this theory only works strictly for a thin lens of constant refractive index, it explains well both the known experimental data [26] and the ray-tracing results described here.

It should be noted that the variation of the lens parameters as a function of accommodation taken from Dubbelmann *et al.*'s work [13] did not consider the effects of the lead and lag of accommodation. Therefore, a potential source of error might affect the horizontal axis of Figs. 3 and 4. A shift toward less values would occur in case of a lag of accommodation (especially significant for higher values of the accommodative stimulus) or toward higher values in case of a lead of accommodation (more significant at a relaxation state of accommodation).

### B. Change of Aberrations with Age

From the previous analysis of accommodation, it is clear that an increase in lens curvature induces negative SA. In the human eye, the unaccommodated crystalline lens also becomes more curved as a consequence of aging. However, this is not associated with a general focal shift in the myopic direction. This situation is called "the lens paradox." When the increase of lens curvature is combined with additional changes in the aging lens (like an increase in lens thickness and a decrease of

the equivalent refractive index), there seems to be a balance of the refractive power, so that it remains approximately stable with age.

It is also well established that the value of ocular SA in the general population does not decrease with age, but rather tends to increase. We may call this a second type of lens paradox that concerns the change of SA with age. In order to solve it, we first combined the variation of lens thickness and equivalent refractive index with the change in lens curvatures, expecting a positive variation. However, this was not the case [see Fig. 6(a), thick line]. The SA from the models consistently changed on the negative direction, indicating that the strong increment of SA induced by the lens curvatures was not cancelled out at all by the changes in thickness and effective index. Next, we checked if lens asphericity changes associated with aging could explain the increase in SA, but *in vivo* experimental data are still scarce in the literature. Only Dubbelman and Van der Heijde's data showed a positive change of the conic constant with age (although it was not statistically significant) [12]. When these values were incorporated into the models, the SA became effectively positive but exceeded by far the experimental results [Fig. 6(b)]. Therefore, an increase in the lens surfaces asphericities with age may explain the positive change in SA observed empirically, but since the rates of increase per year are still unclear (and difficult to measure with the current imaging techniques) we could only make an estimation to fit both variables. As an example, using half of the changes in asphericity measured by Dubbelman *et al.*, the predicted data fitted much better the experimental results (Fig. 6, dashed lines). In addition, the possibility that an age-related variation of the gradient index profile of the lens may also contribute to the referred increment of SA should not be neglected. However, the problem is highly complex and the experimental data in this field are even scarcer (for a recent update, see [36,37]). Also, a recent paper by Campbell presented a shell nested crystalline lens model that predicts the shapes of the shells at different ages [38]. The model estimates changes in lens surfaces asphericities with age but the results were in the negative direction, contrary to Dubbelman *et al.*'s measurements. If Campbell's model is correct (in opposition to Dubbelman *et al.*'s measurements) a more important role of the gradient index should be expected. However, another attempt [39] to model the average lens gradient index as a function of accommodation and age only reported a relatively modest contribution of the gradient index with respect to the lens surfaces asphericities as a source of lens SA (it should be noticed that this publication had the opposite nomenclature for positive/negative SA). This controversy reflects the experimental complications to get access to the internal structures of the eye in a noninvasive manner.

Most of the previous discussion applied also to the modification of the magnitude of coma with age (Fig. 7), although adding asphericity had less impact in the variation of coma than in the case of SA. This could be explained by the fact that the crystalline lens is placed next to the exit pupil of the optical system. In that case, coma should not be affected by the lens conic constant, although we could not neglect the possibility that the posterior lens surface, positioned away from the stop, had a more significant contribution. It should also be noticed that, for the purpose of comparison with other studies, Fig. 7 shows the average change in the magnitude of coma, but not in the Cartesian components of coma. In fact, when the models changed the lens curvatures without adding asphericity (prediction 1), there was a positive change in horizontal coma of about $0.05\,\mu$m (from more negative to less negative values of coma, making the rms decrease) and nearly no changes in vertical coma. This effect was the only consequence of changing the crystalline lens shape factor with age. Adding some positive variation of asphericity, as shown in prediction 3 [Fig. 7(a)] made the ratio of coma per year to increase.

## 5. CONCLUSIONS

A direct relationship between the optical and geometrical changes of the eye during accommodation and aging was demonstrated by using personalized optical models of the human eye. The variation in surface curvature during accommodation induced a negative change in SA similar to values reported in the literature. Changes in lens asphericity generated also some negative shift in SA but much less than the curvature. However, aging effects in coma and SA could not be reproduced with curvature, thickness, and equivalent refractive index changes alone. Adding some changes in asphericity with age would make predictions very close to the measurements, although those changes are still difficult to identify and measured with the current imaging techniques. Better understanding of the variation of the ocular geometry with age and accommodation and their impact in image quality would help the development of optimized optical solutions.

## ACKNOWLEDGMENTS

This work has been supported by Ministerio de Ciencia e Innovación, Spain (grants FIS2007-64765, FIS2010-14926, CONSOLIDER-INGENIO 2010, and CSD2007-00013) and Fundación Séneca (Region de Murcia, Spain), grant 4524/GERM/06.

## REFERENCES

1. S. G. El Hage and F. Berny, "Contribution of crystalline lens to the spherical aberration of the eye," J. Opt. Soc. Am. **63**, 205–211 (1973).
2. P. Artal and A. Guirao, "Contribution of cornea and lens to the aberrations of the human eye," Opt. Lett. **23**, 1713–1715 (1998).
3. P. Artal, A. Guirao, E. Berrio, and D. R. Williams, "Compensation of corneal aberrations by internal optics in the human eye," J. Vision **1**, 1–8 (2001).
4. J. E. Kelly, T. Mihashi, and H. C. Howland, "Compensation of corneal horizontal/vertical astigmatism, lateral coma, and spherical aberration by internal optics of the eye," J. Vision **4**, 262–271 (2004).
5. P. Artal, A. Benito, and J. Tabernero, "The human eye is an example of robust optical design," J. Vision **6**, 1–7 (2006).
6. P. Artal and J. Tabernero, "The eye's aplanatic answer," Nat. Photonics **2**, 586–589 (2008).
7. J. Tabernero, A. Benito, E. Alcón, and P. Artal, "Mechanism of compensation of aberrations in the human eye," J. Opt. Soc. Am. A **24**, 3274–3283 (2007).
8. A. Benito, M. Redondo, and P. Artal, "Laser in situ keratomileusis disrupts the aberration compensation mechanism in the human eye," Am. J. Ophthalmol. **147**, 424–431 (2009).
9. A. Guirao, M. Redondo, E. Geraghty, P. Piers, S. Norrby, and P. Artal, "Corneal optical aberrations and retinal image quality in patients in whom monofocal intraocular lenses were implanted," Arch. Ophthalmol. **120**, 1143–1151 (2002).
10. J. Tabernero, P. Piers, and P. Artal, "Intraocular lens to correct corneal coma," Opt. Lett. **32**, 406–408 (2007).

11. D. A. Atchison, E. Markwell, S. Kasturirangan, J. M. Pope, G. Smith, and P. G. Swann, "Age-related changes in optical and biometric characteristics of emmetropic eyes," J. Vision **8**, 1–20 (2008).
12. M. Dubbelman and G. L. Van der Heijde, "The shape of the aging human lens: curvature, equivalent refractive index and the lens paradox," Vision Res. **41**, 1867–1877 (2001).
13. M. Dubbelman, G. L. Van der Heijde, and H. A. Weeber, "Change in shape of the aging human crystalline lens with accommodation," Vision Res. **45**, 117–132 (2005).
14. M. Dubbelman, G. L. Van der Heijde, and H. A. Weeber, "The thickness of the aging human lens obtained from corrected scheimpflug images," Opt. Vis. Sci. **78**, 411–416 (2001).
15. M. Dubbleman, V. A. D. P. Sicam, and G. L. Van der Heijde, "The shape of the anterior and posterior surface of the aging human cornea," Vision Res. **46**, 993–1001 (2006).
16. P. Artal, M. Ferro, I. Miranda, and R. Navarro, "Effects of aging in retinal image quality," J. Opt. Soc. Am. A **10**, 1656–1662 (1993).
17. A. Guirao, C. Gonzalez, M. Redondo, E. Geraghty, S. Norrby, and P. Artal, "Average optical performance of the human eye as a function of age in a normal population," Invest. Ophthalmol. Visual Sci. **40**, 203–213 (1999).
18. R. I. Calver, M. J. Cox, and D. B. Elliot, "Effect of aging on the monochromatic aberrations of the human eye," J. Opt. Soc. Am. A **16**, 2069–2078 (1999).
19. J. S. McLellan, S. Marcos, and S. A. Burns, "Age-related changes in monochromatic wave aberrations of the human eye," Invest. Ophthalmol. Visual Sci. **42**, 1390–1395 (2001).
20. P. Artal, E. Berrio, A. Guirao, and P. Piers, "Contribution of the cornea and internal surfaces to the change of ocular aberrations with age," J. Opt. Soc. Am. A **19**, 137–143 (2002).
21. I. Brunette, J. M. Bueno, M. Parent, H. Hamam, and P. Simonet, "Monochromatic aberrations as a function of age, from childhood to advanced age," Invest. Ophthalmol. Visual Sci. **44**, 5438–5446 (2003).
22. R. A. Applegate, W. J. Donnelly, J. D. Marsack, and D. E. Koenig, "Three-dimensional relationship between high-order root-mean-square wavefront error, pupil diameter, and aging," J. Opt. Soc. Am. A **24**, 578–587 (2007).
23. D. A. Atchison and E. L. Markwell, "Aberration of emmetropic subjects at different ages," Vision Res. **48**, 2224–2231 (2008).
24. E. Berrio, J. Tabernero, and P. Artal, "Optical aberrations and alignment of the eye with age," J. Vision **10**, 34 (2010).
25. P. Artal, E. J. Fernández, and S. Manzanera, "Are optical aberrations during accommodation a significant problem for refractive surgery?" J. Refract. Surg. **18**, S563–S566 (2002).
26. H. Cheng, J. K. Barnett, A. S. Vilupuru, J. D. Marsack, S. Kasthurirangan, R. A. Applegate, and A. Roorda, "A population study in wave aberrations with accommodation," J. Vision **4**, 272–280 (2004).
27. S. Plainis, H. S. Ginis, and A. Pallikaris, "The effect of ocular aberrations on steady-state errors of accommodative response," J. Vision **5**, 466–477 (2005).
28. H. Radhakrishnan and W. N. Charman, "Age-related changes in ocular aberrations with accommodation," J. Vision **7**, 1–21 (2007).
29. J. Tabernero, A. Benito, V. Nourrit, and P. Artal, "Instrument for measuring the misalignments of ocular surfaces," Opt. Express **14**, 10945–10956 (2006).
30. P. M. Prieto, F. Vargas-Martín, S. Goelz, and P. Artal, "Analysis of the performance of the Hartmann-Shack sensor in the human eye," J. Opt. Soc. Am. A **17**, 1388–1398 (2000).
31. Y. Le Grand and S. G. El Hage, *Physiological Optics*, Springer Series in Optical Sciences (Springer-Verlag, 1980).
32. T. Oshika, S. D. Klyce, R. A. Applegate, and H. C. Howland, "Changes in corneal wavefront aberrations with aging," Invest. Ophthalmol. Visual Sci. **40**, 1351–1355 (1999).
33. A. Guirao, M. Redondo, and P. Artal, "Optical aberrations of the human cornea as a function of age," J. Opt. Soc. Am. A **17**, 1697–1702 (2000).
34. R. Navarro, J. Santamaría, and J. Bescós, "Accommodation-dependent model of the human eye with aspherics," J. Opt. Soc. Am. A **2**, 1273–1281 (1985).
35. L. N. Hazra and C. A. Delisle, "Primary aberrations of a thin lens with different object and image space media," J. Opt. Soc. Am. A **15**, 945–953 (1998).
36. S. Kasthurirangan, E. L. Markwell, D. A. Atchison, and J. M. Pope, "In vivo study of changes in refractive index distribution in the human crystalline lens with age and accommodation," Invest. Ophthalmol. Visual Sci. **49**, 2531–2540 (2008).
37. S. Kasthurirangan, E. L. Markwell, D. A. Atchison, and J. M. Pope, "MRI study of the changes in crystalline lens shape with accommodation and aging in humans," J. Vision **11**, 1–16 (2011).
38. C. E. Campbell, "Nested shell optical model of the lens of the human eye," J. Opt. Soc. Am. A **27**, 2432–2441 (2010).
39. R. Navarro, F. Palos, and L. M. González, "Adaptive model of the gradient index of the human lens. II. Optics of the accommodating aging lens," J. Opt. Soc. Am. A **24**, 2911–2920 (2007).